

Optical properties of highly faceted ZnO rods

A. B. Djurišić^{a)}

Department of Physics, The University of Hong Kong, Pokfulam Road, Hong Kong

W. M. Kwok, W. K. Chan, and D. L. Phillips

Department of Chemistry, The University of Hong Kong, Pokfulam Road, Hong Kong

Y. H. Leung and M. H. Xie

Department of Physics, The University of Hong Kong, Pokfulam Road, Hong Kong

H. Y. Chen, C. L. Wu, and S. Gwo

Department of Physics, National Tsing Hua University, 101, Section 2, Kuang-Fu Road, Hsinchu 300, Taiwan

(Received 22 July 2005; accepted 15 December 2005; published online 13 February 2006)

Highly faceted ZnO rods with 18 side surfaces were synthesized. Their optical properties were characterized by variable temperature photoluminescence, time-resolved photoluminescence, and time-integrated photoluminescence. Low-temperature photoluminescence is dominated by a narrow donor bound exciton peak, while at room temperature ultraviolet emission and green emission can be observed. In spite of the presence of the defect emission, the samples have excellent crystal quality based on the long lifetime of spontaneous emission, with the time constants of biexponential decay equal to 116 ps and 1.2 ns. With increasing pump fluence, stimulated emissions due to excitonic and electron-hole plasma effects were observed. The lasing dynamics in both emission regimes is discussed. © 2006 American Institute of Physics. [DOI: 10.1063/1.2170417]

I. INTRODUCTION

Zinc oxide (ZnO) is a material of great interest for photonic applications. It has a wide band gap of ~ 3.3 eV and a large exciton binding energy of 60 meV. Due to the large exciton binding energy, excitonic lasing at room temperature is possible. The stimulated emission in different morphologies of ZnO has been studied.^{1–21} In particular, lasing in ZnO structures with reduced dimensionality is of interest due to the expected lower threshold power density required for lasing.¹ Lasing has been reported in nanowires,^{1,17,18} nanorod arrays,^{2,3,10} thin films,^{3–5,7,11–14} nanocoral reefs and nanofibers,⁶ microtubes,⁸ tetrapod nanowires,⁹ nanowhiskers,¹⁵ nanoribbons,^{16,19} tetrapods,²⁰ and powder.²¹ Two lasing mechanisms have been identified—random lasing where gain is provided by multiple scatterings and lasing in Fabry-Pérot resonator formed by a nanostructure, bounded by two parallel crystal facets. Random lasing was reported for ZnO nanorod arrays,^{2,3} thin films,^{3,7} and nanowires.¹⁷ However, random lasing mechanism is clearly inconsistent with the lasing from single nanostructures^{16,18–20} and nanostructures with very low density.⁹

Low-temperature photoluminescence was also used to characterize a variety of morphologies of ZnO.^{22–39} Low-temperature photoluminescence measurements of different nanostructures, such as nanowire/nanowall systems,²² nanosheets,²³ nanowires,²⁴ nanorods,^{25,27,29} and nanoblades and nanoflowers,³⁰ were reported. 11 bound exciton transitions have been identified in the low-temperature photoluminescence spectra of ZnO.³⁷ Since the relative intensity of the peaks varies from sample to sample due to variations in

donor/acceptor concentrations and their capture cross sections,³⁸ low-temperature photoluminescence represents a useful tool for evaluation of optical and structural properties of ZnO. Useful information on the crystalline quality and native defects can also be obtained from the linewidths of the peaks in the low-temperature spectrum, as well as their evolution with temperature. Therefore, in this work we combine the variable temperature photoluminescence with the time-resolved photoluminescence to study the optical properties of highly faceted ZnO rods. While the lasing in various ZnO morphologies has been studied as a function of pump fluence, the time-resolved studies of the lasing in ZnO have been scarce.^{5,9,14,15,19,20} In addition, the time evolution of the lasing spectra has been studied only on thin films⁵ and tetrapod nanowires.⁹ In this work, we present a detailed study of the optical properties of highly faceted ZnO rods. This includes the time-resolved photoluminescence studies of spontaneous emission, as well as stimulated emission in exciton-exciton scattering ($E-E$) and electron-hole plasma (EHP) regimes. Spontaneous emission was found to decay biexponentially, similar to previous reports on ZnO nanowires,¹ but with longer decay times of 116 ps and 1.2 ns. The decay times for stimulated emission in both emission regimes were about 4–5 ps. The ultrafast dynamics of the stimulated emission is discussed in detail.

II. EXPERIMENTAL DETAILS

Highly faceted ZnO rods were synthesized by evaporation of Zn powder (Aldrich, 99.999% purity) at 500 °C. The rods were grown on a Si (100) substrate which was placed on the top of the quartz crucible containing Zn powder. Rotary pump was used to evacuate the tube furnace, and then Ar

^{a)}Electronic mail: dalek@hkusua.hku.hk

flow of 0.1 Lpm was introduced. After 500 °C was reached, oxygen gas was added at a flow rate of 0.01 Lpm. After 60 min, the oxygen supply and the furnace were switched off, and the system was left to cool down to room temperature. The morphology of the obtained nanostructures was examined by scanning electron microscopy (SEM) using Carl Zeiss field-emission SEM and Leo 1530 field-emission SEM. Photoluminescence (PL) was measured at different temperatures (7 K room temperature) using a HeCd laser excitation source (325 nm). Time-resolved photoluminescence (TRPL) was measured for 320 nm excitation using the Kerr-gated fluorescence technique, which has been described in detail elsewhere.⁴⁰ Time-integrated photoluminescence (TIPL) was measured for different excitation powers using 1 ps excitation pulses at 267 nm.

III. RESULTS AND DISCUSSION

Figure 1 shows the SEM images of the obtained ZnO nanostructures. Figure 1(a) shows the low magnification image of the obtained structures, while higher magnification images of the representative morphologies are given in Figs. 1(b)–(d). The substrate contains some large pyramids and highly faceted rods. The highly faceted rods have 18 side surfaces. The discussion of the growth mechanism is reported elsewhere.^{41,42}

Figure 2 shows the PL spectra of the highly faceted rods as a function of temperature. The spectrum at 7 K is dominated by a bound exciton peak, located at 3.3628 eV which corresponds to the donor bound I_4 exciton line.^{37,38} The donor responsible for the I_4 line was previously identified as hydrogen.^{34,37} The linewidth of the peak is ~ 7 meV, which is comparable to that in ZnO films grown by metal-organic chemical-vapor deposition technique.³⁶ Even though the obtained results are comparable to those reported for epitaxial layers, narrower peaks (1–3 meV) were reported for aligned ZnO rods^{25,27} and ZnO layers grown by metal-organic vapor-phase epitaxy.³¹ Two of these reports reported the linewidth of bound exciton peaks at 4.2 K, so narrower peaks are partly due to the lower temperature. However, it is also possible that lower variation in size and morphology in the aligned ZnO nanorods^{25,27} plays a role in more narrow bound exciton peak reported for these structures. In addition to dominant donor bound exciton peak, two very small features can be observed at ~ 3.332 and 3.308 eV in the 7 K PL spectrum. The peak at 3.332 eV can most likely be identified as the two-electron satellite of the donor bound exciton.^{25,37} This peak is separated from the I_4 line by a 31 meV, which is in agreement with previously reported values of 34 meV (Ref. 37) and 30 meV.³² The peak at 3.308 eV is possibly a longitudinal-optical (LO)-phonon replica of the free exciton emission since it increases with temperature and it is located at 70 meV lower energy (which corresponds to LO-phonon energy in ZnO)^{25,38} from the free exciton peak which becomes resolvable at ~ 60 K. The weak shoulder on the high-energy side is present at lower temperatures, while at 60 K we can clearly resolve both the first- and second-order phonon replicas. Phonon replicas can be observed up to 210 K, while the bound exciton can be resolved up to ~ 100 K. No

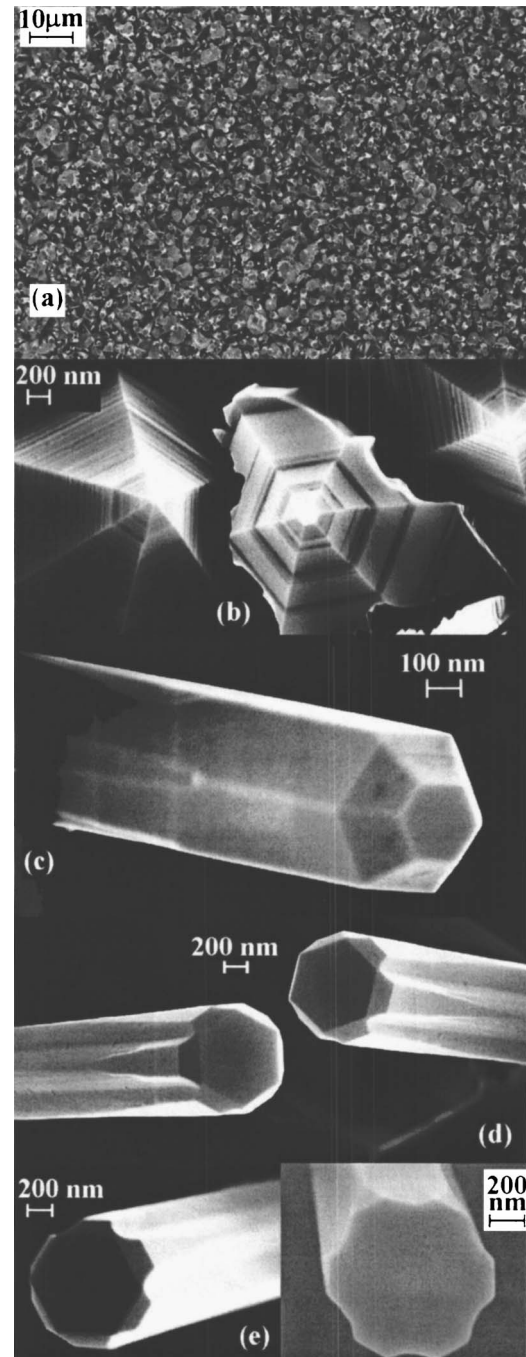


FIG. 1. Representative SEM images of the different shapes of ZnO rods grown on Si substrates.

evidence of surface exciton at ~ 3.3665 eV, which was reported to vanish at 20 K,²² was found in the low-temperature spectra.

Figure 3 shows the comparison between the wide spectral range PL spectra at 10 K and room temperature (RT). The inset shows an enlarged ultraviolet (UV) part of the 10 K PL spectrum as a function of energy. At 10 K, the spectrum is dominated by a strong bound exciton emission, while weak two-electron satellites and LO-phonon replicas can also be observed. Very tiny peak at ~ 3.217 eV could be either an LO-phonon replica or donor-acceptor pair transition, since both of these transitions are in the spectral range of ~ 3.216 – 3.223 eV. No green defect emission can be ob-

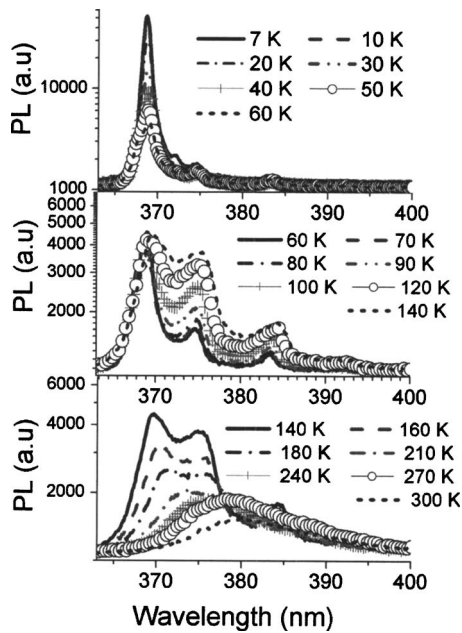


FIG. 2. Photoluminescence spectra at different temperatures.

served at 10 K. The absence of green emission at low temperature indicates that the samples have very good crystalline quality. This is similar to the results reported for aligned ZnO rods.²⁵ Green deep-level emissions at temperatures as low as 6 K were reported for ZnO nanowires.²⁴ At RT, we can observe both the UV emission and the green defect emission. The origin of the green defect emission is highly controversial and numerous hypotheses have been proposed to explain this emission.²⁶ It was shown recently that the green emission originated from surface defects, but the nature of the defect is still not fully clear.²⁶

It was proposed that the existence of green emission may hinder the lasing in ZnO.⁶ However, it was also reported that the ratio of UV to green emission increases as the excitation power increases,²⁶ so that the existence of the defect emission may affect the threshold power but it would not necessarily prevent lasing. In spite of the existence of the defect emission at room temperature, when the samples are excited by femtosecond or picosecond laser pulses, stimulated emission is observed. The obtained integrated photoluminescence spectra are shown in Fig. 4(a). The appearance of narrow

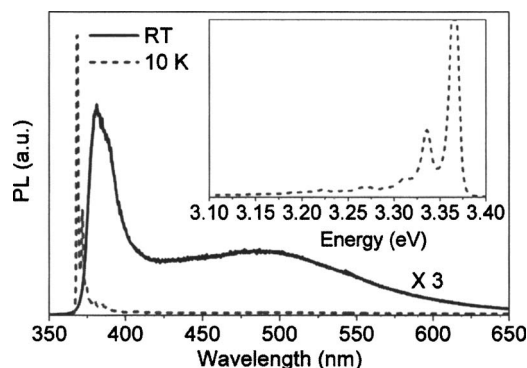


FIG. 3. Comparison between the room-temperature and 10 K photoluminescence spectra. The inset shows the enlarged UV emission at 10 K as a function of energy.

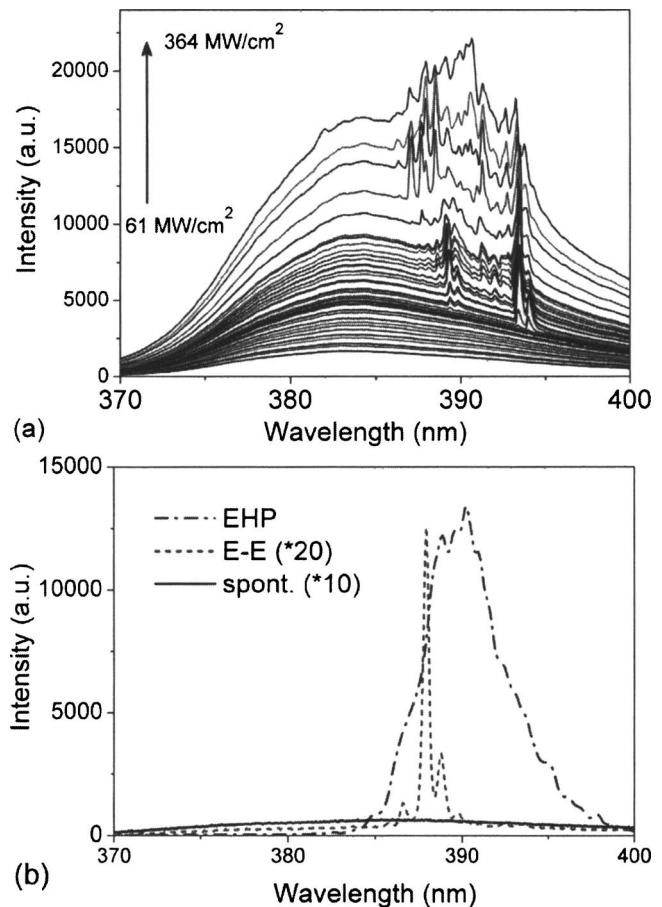


FIG. 4. (a) TIPL spectra at different excitation powers, excited at 267 nm, and pulse duration of 1 ps. The excitation powers are 61, 67, 73, 79, 85, 91, 97, 103, 109, 115, 121, 127, 133, 139, 143, 145, 152, 159, 164, 170, 176, 182, 188, 194, 200, 206, 218, 242, 273, 303, 327, and 364 MW/cm²; (b) TRPL spectra for spontaneous emission (at 1 ps), *E-E* emission (at 11 ps), and EHP emission (at 1.5 ps).

lasing modes can be clearly observed with increasing excitation power. The lower-intensity lasing modes first appear at $\sim 388\text{--}390$ nm, followed by appearance of strong emission at ~ 395 nm. For high excitation powers, a number of narrow peaks can be observed in the spectral range of 385–395 nm. However, it should be noted that the spontaneous and stimulated emissions in ZnO have very different decay times. The decay time of stimulated emission is typically on the order of a few picoseconds, while for spontaneous emission it is on the order of a nanosecond. Consequently, in spite of the high intensity of the stimulated emission compared to the spontaneous one, it is difficult to clearly resolve the lasing modes in the TIPL spectra. Therefore, TRPL measurements excited by 300 fs laser pulses were measured.

Spectra obtained at different times for excitation densities corresponding to spontaneous emission and stimulated emissions in *E-E* and EHP modes are shown in Fig. 4(b). The appearance of narrow lasing modes in the *E-E* regime, as well as the appearance of more broad but highly intense redshifted peaks corresponding to the EHP emission, is obvious. Under femtosecond laser excitation, the threshold for the appearance of narrow lasing modes is $\sim 45 \mu\text{J}/\text{cm}^2$. The mode width is 0.4–0.5 nm, which is significantly lower compared to the spontaneous emission peak width of ~ 17 nm.

Four lasing modes can be observed in the PL spectra shown in Fig. 4(b). Since the modes do not show equal spacing, they likely originate from multiple lasing rods instead of being multiple modes of a single Fabry-Pérot resonator. The lasing modes are positioned at longer wavelengths (lower energy) compared to the spontaneous emission, as would be expected for the exciton-exciton scattering process. The peak position E_n resulting from an exciton-exciton collision process where one of the excitons was scattered to the n th exciton level is given by^{11,21}

$$E_n = E_{\text{ex}} - E_{\text{ex}}^b(1 - 1/n^2) - 3/2kT, \quad (1)$$

where $n=2,3,\dots,\infty$ and $E_{\text{ex}}^b=60$ meV is the exciton binding energy. Therefore, E_n is always lower than E_{ex} . Since the samples represent ensembles of different nanostructures, it is difficult to predict exact peak positions from Eq. (1) since there are variations in the measured spectra for measurements performed at different positions, which are likely due to different values of E_{ex} for different nanostructures. The length of the highly faceted rods studied here is typically in the range of 3–4 μm . It was reported previously for ZnO nanoribbons that the ribbons shorter than ~ 6 μm could not support lasing.¹⁶ The threshold gain can be expressed as¹⁶

$$g_{\text{th}} = \alpha + \frac{1}{2L} \ln^{-1}(R_1 R_2), \quad (2)$$

where L is the length, α is the absorption loss, and R_1 and R_2 are the mirror reflectivities, which are expected to be ~ 0.19 for the ZnO-air interface. For a 4- μm -long rod, if the absorption losses are disregarded, the value of gain as high as $\sim 4 \times 10^4 \text{ cm}^{-1}$ is required to achieve stimulated emission. Therefore, clear observation of stimulated emission indicates possible high gain in these structures. It should be noted that the crystalline quality of the samples is very good, based on the widths of the donor bound exciton emissions obtained at low temperatures and decay times of spontaneous emission at room temperature which are comparable to those of good quality ZnO epitaxial layers. Therefore, one possible reason for the expected high gain in these structures is their good crystalline quality. However, studies of stimulated emission on individual rods instead of rod ensembles are necessary for more precise estimation of the ranges of gain that can be achieved in these nanostructures. When the excitation power is further increased, an intense, broad, and redshifted emission peak is observed, which can be attributed to the lasing in EHP regime. The EHP emission is redshifted compared to the E - E emissions due to the band-gap renormalization.^{4,5,11,13,19–21} The obtained threshold for the EHP emission under femtosecond laser excitation is $90 \mu\text{J}/\text{cm}^2$.

We also performed detailed time-resolved measurements in order to study the ultrafast dynamics of the spontaneous and stimulated emissions. The obtained results are shown in Fig. 5. The spontaneous emission shows biexponential decay, in agreement with the previous reports.^{1,31,43} The obtained time constants, 116 ps and 1.2 ns, are larger than those reported for ZnO nanowires (70 ps and 350 ps).¹ The slow decay of the spontaneous emission in highly faceted rods indicates their excellent crystal quality. Compared to other

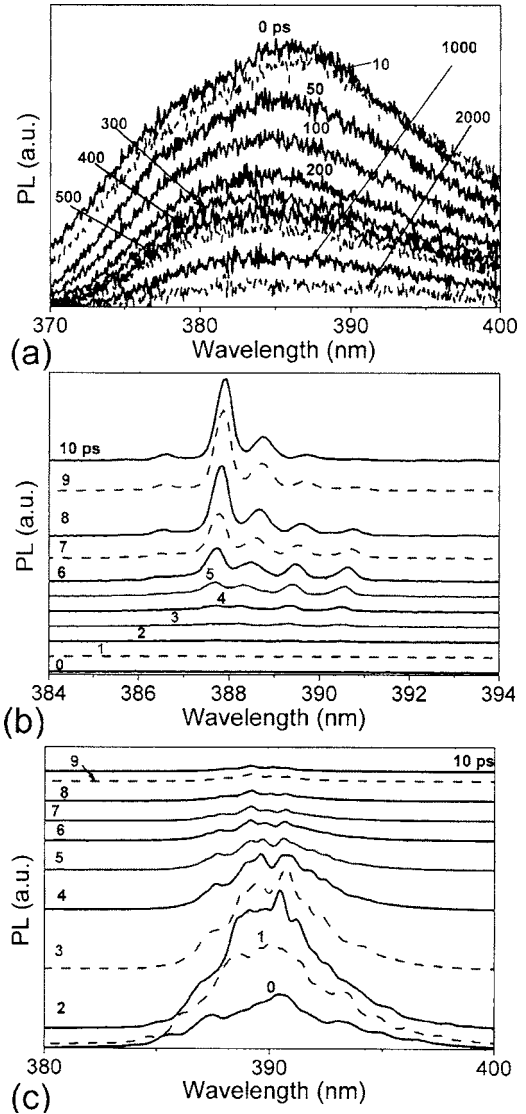


FIG. 5. Time-resolved PL spectra for (a) spontaneous emission, (b) stimulated emission due to exciton-exciton scattering, and (c) stimulated emission due to EHP. The curves for E - E and EHP emissions have been vertically shifted to improve clarity.

reports in the literature, the time constants of emission from highly faceted rods are larger (36–110 ps) (Refs. 44 and 45) and comparable to those reported for ZnO epitaxial layers (180 ps and 1.0 ns),³¹ as well as nanorods with length over 600 nm (190 ps and 1.4 ns).⁴³

The time-resolved spectra corresponding to the lasing in E - E regime are shown in Fig. 5(b). It can be observed that the lasing modes are narrow, with linewidth of 0.4–0.5 nm. Therefore, both the threshold power and the linewidth are lower than those of hexagonal ZnO nanowhiskers.¹⁵ The obtained linewidth is somewhat larger than that of aligned nanowire/nanorod arrays,^{1,10} and some of the single nanostructures,^{16,18} but smaller than the commonly reported lasing mode width in ensembles of ZnO nano- and microstructures.^{8,9,15} It can be observed that there is considerable delay time (>5 ps) until the lasing modes begin to be clearly resolved. The longer delay times for E - E emission in ZnO nanostructures were attributed to the longer time needed to achieve a high concentration of excitons in the

excited state.¹⁹ The decay times were 4–5 ps. The modes were not equally spaced, as expected for lasing from an ensemble of the nanostructures.

Figure 5(c) shows the time-resolved lasing spectra in the EHP regime. The EHP emissions shows short (~ 2 ps) rising time and 2–3 ps decay time. Fast rising time of the EHP emission is in agreement with the previous reports.^{5,9,19,20} The rise time of the EHP emission is related to the formation of the electron-hole plasma by thermalization of the hot carriers.^{19,20} The decay time of the EHP emission is also fast, and decay constants as low as 1.1 ps (for ZnO tetrapods)²⁰ were previously reported. No significant peak shifts with time can be observed, unlike the behavior of the EHP emission in ZnO thin films, where redshift followed by blueshift was reported with increasing time.⁵ It can be observed that, with increasing time, more sharp features can be observed in the broad emission peak. The presence of sharp peaks was reported previously for lasing from ZnO nanocrystalline powder.²¹ The presence of sharp peaks could be associated with the random lasing or donor-acceptor pair (DAP) emission.²¹ However, based on the low-temperature photoluminescence of our samples, sharp DAP lines would not be very likely. Random lasing was identified as a gain mechanism in ZnO nanowires.¹⁷ However, Fourier transform of the lasing spectrum measured does not reveal harmonics which would be consistent with the random lasing assumption.¹⁷ It is also possible that the emergence of the sharp features is due to the coexistence of lasing in *E-E* and EHP modes. This would be in agreement with the previous report on coexistence of *E-E* and EHP emissions in ZnO thin films due to spatial uniformity of the sample.¹⁴ Since our samples represent an ensemble of ZnO rods, spatial nonuniformity is unavoidable. Also, EHP emission is expected to occur for carrier densities above Mott density ($\sim 4 \times 10^{18}$ in ZnO).¹⁸ As the time increases the free-carrier concentration is reduced due to radiative recombination, which could result in the coexistence of excitonic and EHP effects.

IV. CONCLUSIONS

Optical properties of highly faceted ZnO rods were studied by variable temperature photoluminescence, time-resolved photoluminescence, and time-integrated photoluminescence. The low-temperature photoluminescence spectrum was dominated by a donor-bound exciton transition. At room temperature, both UV and green emissions associated with defects were observed. In spite of the presence of defect emission, long decay times of spontaneous emission (116 ps and 1.2 ns) were obtained, illustrating excellent crystal quality. The samples exhibited stimulated emission due to exciton-exciton scattering with a threshold of $\sim 45 \mu\text{J}/\text{cm}^2$ and electron-hole plasma with a threshold of $90 \mu\text{J}/\text{cm}^2$. The differences in the evolution of the emission spectra in two lasing regimes were discussed.

ACKNOWLEDGMENT

This work is partly supported by the Research Grant Council of the Hong Kong Special Administrative Region,

China (Project Nos. HKU 1/01C and HKU/7021/03P to DLP and HKU 7019/04P to ABD).

- ¹M. H. Huang *et al.*, *Science* **292**, 1897 (2001).
- ²S. F. Yu, C. Yuen, S. P. Lau, W. I. Park, and G.-C. Yi, *Appl. Phys. Lett.* **84**, 3241 (2004).
- ³X. Liu, A. Yamilov, X. Wu, J.-G. Zheng, H. Cao, and R. P. H. Chang, *Chem. Mater.* **16**, 5414 (2004).
- ⁴A. Yamamoto, T. Kido, T. Goto, Y. Chen, T. Yao, and A. Kasuya, *J. Cryst. Growth* **214/215**, 308 (2000).
- ⁵J. Takeda, S. Kurita, Y. Chen, and T. Yao, *Int. J. Mod. Phys. B* **15**, 3669 (2001).
- ⁶J.-H. Choy, E.-S. Jang, J.-H. Won, J.-H. Chung, D.-J. Jang, and Y.-W. Kim, *Appl. Phys. Lett.* **84**, 287 (2004).
- ⁷H. Cao, Y. G. Zhao, H. C. Ong, S. T. Ho, J. Y. Dai, J. Y. Wu, and R. P. H. Chang, *Appl. Phys. Lett.* **73**, 3656 (1998).
- ⁸X. W. Sun, S. F. Yu, C. X. Xu, C. Yuen, B. J. Chen, and S. Li, *Jpn. J. Appl. Phys., Part 2* **42**, L1229 (2003).
- ⁹Y. H. Leung, W. M. Kwok, A. B. Djurišić, D. L. Phillips, and W. K. Chan, *Nanotechnology* **16**, 579 (2005).
- ¹⁰J.-H. Choy, E.-S. Jang, J.-H. Won, J.-H. Chung, D.-J. Jang, and Y.-W. Kim, *Adv. Mater. (Weinheim, Ger.)* **15**, 1911 (2003).
- ¹¹P. Zu, Z. K. Tang, G. K. L. Wong, M. Kawasaki, A. Ohtomo, H. Koinuma, and Y. Segawa, *Solid State Commun.* **103**, 459 (1997).
- ¹²Z. K. Tang, G. K. L. Wong, P. Yu, M. Kawasaki, A. Ohtomo, H. Koinuma, and Y. Segawa, *Appl. Phys. Lett.* **72**, 3270 (1998).
- ¹³D. M. Bagnall, Y. F. Chen, M. Y. Shen, Z. Zhu, T. Goto, and T. Yao, *J. Cryst. Growth* **184/185**, 605 (1998).
- ¹⁴Ü. Özgür, A. Teke, C. Liu, S.-J. Cho, H. Morkoç, and H. O. Everitt, *Appl. Phys. Lett.* **84**, 3223 (2004).
- ¹⁵Z. Qiu, K. S. Wong, M. Wu, W. Lin, and H. Xu, *Appl. Phys. Lett.* **84**, 2739 (2004).
- ¹⁶H. Yan *et al.*, *Adv. Mater. (Weinheim, Ger.)* **15**, 1907 (2003).
- ¹⁷H.-C. Hsu, C.-Y. Wu, and W.-F. Hsieh, *J. Appl. Phys.* **97**, 064315 (2005).
- ¹⁸J. C. Johnson, H. Yan, P. Yang, and R. J. Saykally, *J. Phys. Chem. B* **107**, 8816 (2003).
- ¹⁹J. C. Johnson, K. P. Knutsen, H. Yan, M. Law, Y. Zhang, P. Yang, and R. J. Saykally, *Nano Lett.* **4**, 197 (2004).
- ²⁰J. M. Szarko, J. K. Song, C. W. Blackledge, I. Swart, S. R. Leone, S. Li, and Y. Zhao, *Chem. Phys. Lett.* **404**, 171 (2005).
- ²¹Y. Sun, J. B. Ketterson, and G. K. L. Wong, *Appl. Phys. Lett.* **77**, 2322 (2000).
- ²²J. Grabowska, A. Meaney, K. K. Nanda, J.-P. Mosnier, M. O. Henry, J.-R. Duclère, and E. McGlynn, *Phys. Rev. B* **71**, 115439 (2005).
- ²³S. Chen, Y. Liu, C. Shao, R. Mu, Y. Lu, J. Zhang, D. Shen, and X. Fan, *Adv. Mater. (Weinheim, Ger.)* **17**, 586 (2005).
- ²⁴H.-C. Hsu and W.-F. Hsieh, *Solid State Commun.* **131**, 371 (2004).
- ²⁵B. P. Zhang, N. T. Binh, Y. Segawa, K. Wakatsuki, and N. Usami, *Appl. Phys. Lett.* **83**, 1635 (2003).
- ²⁶A. B. Djurišić *et al.*, *Adv. Funct. Mater.* **14**, 856 (2004).
- ²⁷W. I. Park, Y. H. Jun, S. W. Jung, and G.-C. Yi, *Appl. Phys. Lett.* **82**, 964 (2003).
- ²⁸B. P. Zhang, C. Y. Liu, Y. Segawa, Y. Kashiwaba, and K. Haga, *Thin Solid Films* **474**, 165 (2005).
- ²⁹J. Jie, G. Wang, Y. Chen, X. Han, Q. Wang, B. Xu, and J. G. Hou, *Appl. Phys. Lett.* **86**, 031909 (2005).
- ³⁰H.-W. Suh, G.-Y. Kim, Y.-S. Jung, W.-K. Choi, and D. Byun, *J. Appl. Phys.* **97**, 044305 (2005).
- ³¹S. W. Jung, W. I. Park, H. D. Cheong, G.-C. Yi, H. M. Jang, S. Hong, and T. Joo, *Appl. Phys. Lett.* **80**, 1924 (2002).
- ³²K. Thonke, Th. Gruber, N. Teofilov, R. Schönfelder, A. Waag, and R. Sauer, *Physica B* **308–310**, 945 (2001).
- ³³A. Zeuner, H. Alves, D. M. Hofmann, B. K. Meyer, M. Heuken, J. Blasing, and A. Krost, *Appl. Phys. Lett.* **80**, 2078 (2002).
- ³⁴M. Strassburg *et al.*, *Phys. Status Solidi B* **241**, 607 (2004).
- ³⁵J. Gutowski, N. Presser, and I. Broser, *Phys. Rev. B* **38**, 9746 (1988).
- ³⁶H. Kato, M. Sano, K. Miyamoto, T. Yao, B.-P. Zhang, K. Wakatsuki, and Y. Segawa, *Phys. Status Solidi B* **241**, 2825 (2004).
- ³⁷B. K. Meyer *et al.*, *Phys. Status Solidi B* **241**, 231 (2004).
- ³⁸A. Teke, Ü. Özgür, S. Doğan, X. Gu, H. Morkoç, B. Nemeth, J. Nause, and H. O. Everitt, *Phys. Rev. B* **70**, 195207 (2004).
- ³⁹Y. Zhang, B. Lin, X. Sun, and Z. Fu, *Appl. Phys. Lett.* **86**, 131910 (2005).
- ⁴⁰C. Ma, W. M. Kwok, W. S. Chan, P. Zuo, J. T. W. Kan, P. H. Toy, and D.

- L. Phillips, *J. Am. Chem. Soc.* **127**, 1463 (2005).
- ⁴¹W. M. Kwok *et al.*, *Chem. Phys. Lett.* **412**, 141 (2005).
- ⁴²Y. H. Leung, A. B. Djurišić, and M. H. Xie, *J. Cryst. Growth* **284**, 80 (2005).
- ⁴³S. Hong, T. Joo, W. I. Park, Y. H. Jun, and G.-C. Yi, *Appl. Phys. Lett.* **83**, 4157 (2003).
- ⁴⁴T. Koida, S. F. Chichibu, A. Uedono, A. Tsukazaki, M. Kawasaki, T. Sota, and H. Koinuma, *Appl. Phys. Lett.* **82**, 532 (2003).
- ⁴⁵T. Koida, A. Uedono, A. Tsukazaki, T. Sota, M. Kawasaki, and S. F. Chichibu, *Phys. Status Solidi A* **201**, 2841 (2004).